Generalized Ramsey methods in the spectroscopy of coherent-population-trapping resonances

M. Yu. Basalaev [1,2,3,*] V. I. Yudin [1,2,3,†] D. V. Kovalenko [1,2] T. Zanon-Willette,[4] and A. V. Taichenachev[1,2]

[1]*Institute of Laser Physics SB RAS, Prospekt Akademika Lavrent'eva 15B, Novosibirsk 630090, Russia*
[2]*Novosibirsk State University, Ulica Pirogova 1, Novosibirsk 630090, Russia*
[3]*Novosibirsk State Technical University, Prospekt Karla Marksa 20, Novosibirsk 630073, Russia*
[4]*Sorbonne Université, Observatoire de Paris, Université PSL, CNRS, LERMA, F-75005 Paris, France*

We present a rigorous justification for the applicability of the recently developed methods of generalized autobalanced Ramsey spectroscopy (GABRS) [V. I. Yudin *et al.*, Phys. Rev. Appl. **9**, 054034 (2018)] and combined error signal in Ramsey spectroscopy (CESRS) [V. I. Yudin *et al.*, New J. Phys. **20**, 123016 (2018)] for resonances of coherent population trapping (CPT). A protocol of modified combined error signal for CPT resonances is also proposed, in which two successive interrogations of atoms under different times of free evolution are integrated in one cycle. The implementation of the GABRS and CESRS methods in a compact atomic clock based on the CPT effect allows us to significantly suppress the light shift and its fluctuation, which will lead to an improvement in the long-term stability and accuracy of these devices. Moreover, these spectroscopic schemes are insensitive to various distortions of the pulse shape, relaxation processes, errors in the generation of phase jumps, etc., which provides their high reliability and immunity to perturbations.

I. INTRODUCTION

Atomic clocks are quantum devices that provide high-precision measurements of frequency and time [1–5] for solving fundamental and applied problems. In particular, they are used in such important areas as satellite and inertial navigation, synchronization of telecommunication networks, secure data transfer, geodesy, verification of fundamental physical theories, etc. [6–11].

Great successes in the development of small-size microwave atomic clocks have been achieved with the use of coherent-population-trapping (CPT) resonances [12–16] to stabilize the frequency of a local oscillator (LO). The advantage of such devices consists in the completely optical scheme for the exciting of radio-frequency transition without a microwave resonator. This enables one to significantly reduce the dimension of the physical package (up to the chip-scale) and power consumption [17–19]. The essence of the CPT effect is the following. In the process of interaction with a coherent two-frequency (bichromatic) field, atoms are pumped to the so-called dark state which does not absorb the light field. This state is formed when the difference of optical frequencies varies near the hyperfine splitting of the ground state, which leads to the appearance of a narrow dip (peak) in the absorption (transmission) spectrum. The width and the amplitude of this resonance are determined by the pumping rate, which depends on the field intensity and atomic relaxation parameters. The use of optical cells with a buffer gas or an antirelaxation coating allows one to significantly

reduce the resonance width, which is usually of the order of 0.1–1 kHz.

Spectroscopic measurements during the frequency stabilization are accompanied by a perturbation of clock transition frequency due to the ac-Stark effect. This light shift depends on the intensity and frequency of the optical fields and is one of the key factors limiting the metrological characteristics (stability and accuracy) of atomic clocks. In the optical frequency standards, great progress in suppressing the light shift has occurred due to the use of Ramsey-type pulsed spectroscopy [20]. It was initiated in Ref. [21], where the method of hyper-Ramsey spectroscopy was proposed. This method is based on the application of two pulses with different durations, while the part of the second pulse has a phase shifted by π (composite pulse). Implementation of the hyper-Ramsey technique made it possible to achieve light shift suppression by several orders of magnitude [22,23]. Further, some modifications of this approach were constructed using various other schemes to generate the error signal for the frequency stabilization [24–28]. Recent advances in suppressing light shift in optical atomic clocks are related to the autobalanced Ramsey spectroscopy technique (ABRS) [29], its generalization (GABRS) [30], and the protocol of combined error signal in Ramsey spectroscopy (CESRS) [31]. These methods are based on the interrogation of atoms by two Ramsey sequences with different times of free evolution (dark times). GABRS uses two feedback loops, one of which serves to adjust the LO frequency, and the other loop drives a concomitant well-controlled parameter associated with Ramsey pulses. With simultaneous stabilization of the LO frequency and the concomitant parameter, the light shift will be suppressed (completely in the ideal case). In Ref. [29], a stabilization scheme was proposed and implemented, where an additional phase shift of the field during the second Ramsey

*mbasalaev@gmail.com
†viyudin@mail.ru

pulse was employed as the concomitant parameter. However, in the theoretical paper [30], it was shown that there are other alternatives for the choosing of the concomitant parameter. In contrast to the GABRS technique, the CESRS protocol [31] uses only one feedback loop. In this approach, the error signal for frequency stabilization is formed by subtracting with the corresponding calibration coefficient two ordinary error signals for each Ramsey sequence.

The implementation of the GABRS and CESRS methods to the microwave atomic clocks based on the CPT resonances seems attractive and very promising. For example, in Refs. [32,33] the ABRS with a correction phase as the concomitant parameter was realized in a CPT-based Cs vapor-cell clock. Here, the relative long-term instability was achieved at the level of several units of 10^{-15}. Also, GABRS and CESRS were recently implemented in experiments with cold Rb atoms [34,35], where the light shift was suppressed by more than an order of magnitude. Despite the fact that the intuitive transfer of the GABRS and CESRS methods to the CPT spectroscopy has demonstrated their efficiency, there was no rigorous justification for such a step. Indeed, the theoretical analysis in the original works [30,31] was carried out within the framework of a two-level atomic model, which is applicable only to optical clocks. However, the physical processes under the simultaneous resonant interaction of a coherent polychromatic field with several transitions in a multilevel atom significantly differ from the excitation of a single optical transition (usually ultranarrow) by a monochromatic field. Therefore, the automatic dissemination of the GABRS and CESRS techniques to CPT resonances is not obvious. To justify this possibility for CPT even in the simplest case, it is necessary to investigate a three-level Λ system interacting with a coherent two-frequency field.

In this paper, we perform rigorous mathematical proof of the applicability of GABRS and CESRS for atomic clocks based on CPT resonance. Moreover, for GABRS, two variants for the choosing of the concomitant parameter are analyzed: the correction phase of the second Ramsey pulse and the additional frequency jump during the action of both Ramsey pulses. Also we consider a modified CESRS, in which two successive interrogations with different times of free evolution are combined in one cycle.

II. THEORETICAL MODEL

As a theoretical model of the atomic medium, we consider a three-level Λ system (see Fig. 1) interacting with the Ramsey pulses of a bichromatic field (see Fig. 2):

$$E(t) = E_1(t)e^{-i(\omega_1 t + \varphi_1)} + E_2(t)e^{-i(\omega_2 t + \varphi_2)} + \text{c.c.} \quad (1)$$

The resonance of coherent population trapping is excited under the condition that the frequency difference $\omega_1 - \omega_2$ is varied near the frequency ω_{hfs} of the transition between the lower states $|1\rangle$ and $|2\rangle$ (clock states). The temporal dynamics of the Λ system we describe using the formalism of the atomic density matrix in the basis of states $\{|j\rangle\}$ (see Fig. 1):

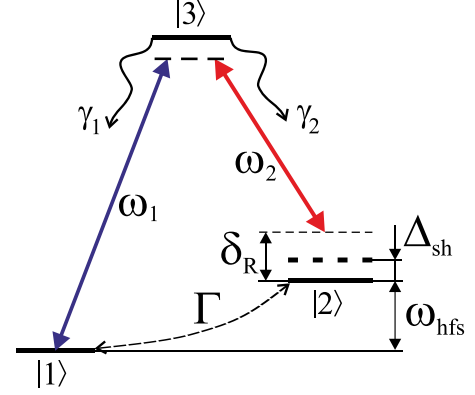$$\hat{\rho}(t) = \sum_{m,n} |m\rangle \rho_{mn}(t)\langle n|. \quad (2)$$

FIG. 1. Energy scheme of the three-level Λ system. Here ω_1 and ω_2 are the frequencies of resonant optical fields; Δ_{sh} is the light (Stark) shift of the clock transition frequency; γ_1 and γ_2 are the rates of spontaneous population transfer from the upper state $|3\rangle$ to the lower states $|1\rangle$ and $|2\rangle$, respectively; and Γ is the decay rate of the coherence between the states $|1\rangle$ and $|2\rangle$.

In principle, the Λ system can be reduced to a two-level model (over the lower states $|1\rangle$ and $|2\rangle$) within the framework of perturbation theory for weak fields. However, from the viewpoint of high-precision metrology, the use of this approximation is not sufficient to estimate the light shifts, because the question of the accuracy of the obtained results will always remain open.

In the rotating-wave approximation, the equations for the density matrix have the following form:

$$\partial_t \rho_{11} = \frac{\Gamma}{2}\text{Tr}\{\hat{\rho}\} - \Gamma\rho_{11} + \gamma_1\rho_{33} - i\Omega_1\rho_{13} + i\Omega_1^*\rho_{31},$$

$$\partial_t \rho_{12} = [-\Gamma - i(\delta_{\text{R}} - \Delta_{\text{sh}})]\rho_{12} + i\Omega_1^*\rho_{32} - i\Omega_2\rho_{13},$$

$$\partial_t \rho_{21} = [-\Gamma + i(\delta_{\text{R}} - \Delta_{\text{sh}})]\rho_{21} - i\Omega_1\rho_{23} + i\Omega_2^*\rho_{31},$$

$$\partial_t \rho_{22} = \frac{\Gamma}{2}\text{Tr}\{\hat{\rho}\} - \Gamma\rho_{22} + \gamma_2\rho_{33} - i\Omega_2\rho_{23} + i\Omega_2^*\rho_{32},$$

$$\partial_t \rho_{13} = (-\gamma_{\text{opt}} - i\delta_1)\rho_{13} - i\Omega_1^*(\rho_{11} - \rho_{33}) - i\Omega_2^*\rho_{12},$$

$$\partial_t \rho_{31} = (-\gamma_{\text{opt}} + i\delta_1)\rho_{31} + i\Omega_1(\rho_{11} - \rho_{33}) + i\Omega_2\rho_{21},$$

$$\partial_t \rho_{23} = (-\gamma_{\text{opt}} - i\delta_2)\rho_{23} - i\Omega_2^*(\rho_{22} - \rho_{33}) - i\Omega_1^*\rho_{21},$$

$$\partial_t \rho_{32} = (-\gamma_{\text{opt}} + i\delta_2)\rho_{32} + i\Omega_2(\rho_{22} - \rho_{33}) + i\Omega_1\rho_{12},$$

$$\partial_t \rho_{33} = -(\gamma_{\text{sp}} + \Gamma)\rho_{33} + i\Omega_1\rho_{13} - i\Omega_1^*\rho_{31} + i\Omega_2\rho_{23} - i\Omega_2^*\rho_{32}.$$
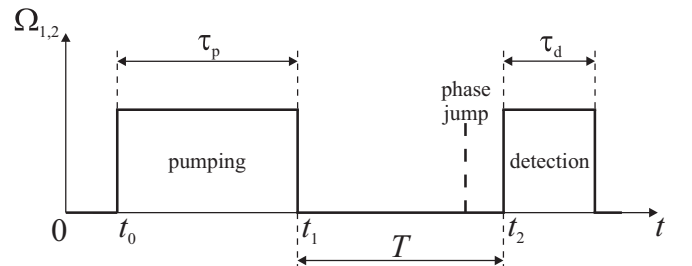
$$(3)$$

FIG. 2. Ramsey scheme for spectroscopy of the CPT resonances. The first pulse pumps atoms into a dark state. The second pulse detects the spectroscopic information.

The notation is introduced in Eq. (3): $\Omega_1 = d_{31}E_1 e^{-i\varphi_1}/\hbar$ and $\Omega_2 = d_{32}E_2 e^{-i\varphi_2}/\hbar$ are Rabi frequencies for transitions $|1\rangle \leftrightarrow |3\rangle$ and $|2\rangle \leftrightarrow |3\rangle$, respectively ($d_{31}$ and d_{32} are the matrix elements of the operator of the electrical dipole moment); $\delta_1 = \omega_1 - \omega_{31}$ and $\delta_2 = \omega_2 - \omega_{32}$ are one-photon detunings of laser fields; $\delta_R = \omega_1 - \omega_2 - \omega_{hfs}$ is two-photon (Raman) detuning; Δ_{sh} is the light (Stark) shift of the clock transition frequency during the Ramsey pulses; γ_{opt} is the decay rate of optical coherences (due to spontaneous decay processes, collisions with buffer gas atoms, etc.); γ_1 and γ_2 are the rates of spontaneous population transfer from state $|3\rangle$ to states $|1\rangle$ and $|2\rangle$, respectively; γ_{sp} is the spontaneous decay rate of the excited state $|3\rangle$ (in the case of a closed Λ system, $\gamma_{sp} = \gamma_1 + \gamma_2$); and the constant Γ models the relaxation of atoms (for example, due to transit effects) to an equilibrium isotropic distribution over the lower levels of the Λ system.

Note that the phenomenological parameter Δ_{sh} is a total far-off-resonant light shift (of the clock transition $|1\rangle \rightarrow |2\rangle$), which arises due to interaction of all frequency components with all off-resonant atomic levels. The possible resonant shifts in the case of $\delta_1 \neq 0$ and/or $\delta_2 \neq 0$ are automatically taken into account in the system of Eqs. (3). The relaxation rate Γ is mainly determined by the transit time τ_{tr} of the atoms through the laser beam ($\Gamma \sim \tau_{tr}^{-1}$). Therefore, collisions with the buffer gas significantly increase τ_{tr} due to the diffusion character of the atomic motion (without destroying the hyperfine coherence), which results in narrowing of the dark resonance [36]. On the other hand, a buffer gas increases considerably the optical dephasing rate $\gamma_{opt} \gg \gamma_{sp}$ [37], while without buffer gas $\gamma_{opt} = \gamma_{sp}/2$.

The system of linear Eqs. (3), can be represented in vector form as

$$\partial_t \vec{\rho} = \hat{L}\vec{\rho}, \qquad (4)$$

where the column vector $\vec{\rho}(t)$ is constructed from the elements of the density matrix $\hat{\rho}(t)$ as follows,

$$\vec{\rho} = (\rho_{11}, \rho_{12}, \rho_{21}, \rho_{22}, \rho_{13}, \rho_{31}, \rho_{23}, \rho_{32}, \rho_{33})^T, \qquad (5)$$

and the matrix $\hat{L}$ (Liouvillian) [see Eq. (A1)] is determined by the coefficients of Eqs. (3).

As a spectroscopic signal, we investigate the absorbtion during the detecting pulse (for $t > t_2$, see Fig. 2), which in the case of an optically thin medium is proportional to

$$A(t) = 2\,\text{Im}\{\Omega_1(t)\rho_{31}(t) + \Omega_2(t)\rho_{32}(t)\}. \qquad (6)$$

The signal accumulated during the detection time τ_d is calculated by integrating the expression (6) over time:

$$\overline{A}(\delta_R) = \int_{t_2}^{t_2+\tau_d} A(t)\,dt. \qquad (7)$$

Using the standard definition of a scalar product

$$(\vec{x}, \vec{y}) = \sum_m x_m^* y_m,$$

the expression (6) can be written as follows:

$$A(t) = (\vec{\Omega}(t), \hat{W}_d(t)\hat{G}_T \hat{W}_p \vec{\rho}_{in}), \qquad (8)$$

where the vector $\vec{\Omega}(t)$ is defined as

$$\vec{\Omega} = (0, 0, 0, 0, -i\Omega_1^*, i\Omega_1, -i\Omega_2^*, i\Omega_2, 0)^T. \qquad (9)$$

The vector $\vec{\rho}_{in}$ corresponds to the initial atomic state. The operators $\hat{W}_p \equiv \hat{W}_p(t_1, t_0)$ and $\hat{W}_d(t) \equiv \hat{W}_d(t, t_2)$ describe the evolution of atoms interacting with a pump pulse ($t_0 < t < t_1$) and a detecting pulse ($t > t_2$), respectively. The operator $\hat{G}_T$ corresponds to the free evolution of atoms ($t_1 \leqslant t \leqslant t_2 = t_1 + T$):

$$\hat{G}_T = e^{\hat{L}_0 T}, \qquad (10)$$

where Liouvillian $\hat{L}_0$ (A2) can be constructed from Eqs. (3)–(5) in the absence of the light field (i.e., $\Omega_1 = \Omega_2 = 0$ and $\Delta_{sh} = 0$). The explicit form of the matrix $\hat{G}_T$ (A3) is given in Appendix A.

The dark period T under real experimental conditions, as a rule, significantly exceeds (by 2–4 orders of magnitude) the decay times of the excited-state population and the optical coherences; i.e., there is a relation $T \gg \gamma_{opt}^{-1}, \gamma_{sp}^{-1}$. Therefore, in the diagonal elements of the matrix $\hat{G}_T$ [see Eq. (A3)], we can accept $e^{-\gamma_{sp}T} \approx 0$ and $e^{-\gamma_{opt}T} \approx 0$. In this case, the operator $\hat{G}_T$ takes the form

$$\hat{G}_T \approx \begin{pmatrix} G_{11} & 0 & 0 & G_{14} & 0 & 0 & 0 & 0 & G_{19} \\ 0 & 0 & e^{-(\Gamma+i\delta_R)T} & 0 & 0 & 0 & 0 & 0 & 0 \\ 0 & 0 & 0 & e^{-(\Gamma-i\delta_R)T} & 0 & 0 & 0 & 0 & 0 \\ G_{41} & 0 & 0 & G_{44} & 0 & 0 & 0 & 0 & G_{49} \\ 0 & 0 & 0 & 0 & 0 & 0 & 0 & 0 & 0 \\ 0 & 0 & 0 & 0 & 0 & 0 & 0 & 0 & 0 \\ 0 & 0 & 0 & 0 & 0 & 0 & 0 & 0 & 0 \\ 0 & 0 & 0 & 0 & 0 & 0 & 0 & 0 & 0 \\ 0 & 0 & 0 & 0 & 0 & 0 & 0 & 0 & 0 \end{pmatrix}. \qquad (11)$$

Let us consider the stabilization scheme, where for generation of the error signal $S_{err}(\delta_R)$ the jumps of the relative phase of the bichromatic field ($\varphi_1 - \varphi_2$) are employed before the second Ramsey pulse. Using the formulas (7) and (8), we write the expression for the spectroscopic signal taking into account the phase jump:

$$\overline{A}(\delta_R, \alpha_1, \alpha_2) = \int_{t_2}^{t_2+\tau_d} (\vec{\Omega}(t), \hat{W}_d(t)\hat{\Phi}(\alpha_1, \alpha_2)\hat{G}_T \hat{W}_p \vec{\rho}_{in})dt, \qquad (12)$$

where the phase jump operator $\hat{\Phi}(\alpha_1, \alpha_2)$ for a bichromatic field has the form

$$
\hat{\Phi}(\alpha_1, \alpha_2) = \begin{pmatrix}
1 & 0 & 0 & 0 & 0 & 0 & 0 & 0 & 0 \\
0 & e^{-i(\alpha_1-\alpha_2)} & 0 & 0 & 0 & 0 & 0 & 0 & 0 \\
0 & 0 & e^{i(\alpha_1-\alpha_2)} & 0 & 0 & 0 & 0 & 0 & 0 \\
0 & 0 & 0 & 1 & 0 & 0 & 0 & 0 & 0 \\
0 & 0 & 0 & 0 & e^{-i\alpha_1} & 0 & 0 & 0 & 0 \\
0 & 0 & 0 & 0 & 0 & e^{i\alpha_1} & 0 & 0 & 0 \\
0 & 0 & 0 & 0 & 0 & 0 & e^{-i\alpha_2} & 0 & 0 \\
0 & 0 & 0 & 0 & 0 & 0 & 0 & e^{i\alpha_2} & 0 \\
0 & 0 & 0 & 0 & 0 & 0 & 0 & 0 & 1
\end{pmatrix}.
\tag{13}
$$

The error signal $S_{\mathrm{err}}(\delta_{\mathrm{R}})$ is formed as the difference of the signals (12) for two different phase jumps:

$$
S_{\mathrm{err}}(\delta_{\mathrm{R}}) = \overline{A}(\delta_{\mathrm{R}}, \alpha_1^+, \alpha_2^+) - \overline{A}(\delta_{\mathrm{R}}, \alpha_1^-, \alpha_2^-) = \int_{t_2}^{t_2+\tau_{\mathrm{d}}} (\vec{\Omega}(t), \hat{W}_{\mathrm{d}}(t)\hat{D}_{\Phi}\hat{G}_T\hat{W}_{\mathrm{p}}\vec{\rho}_{\mathrm{in}})dt,
\tag{14}
$$

where the upper index "+" indicates the first phase jump, and the index "−" corresponds to the second phase jump. The operator $\hat{D}_{\Phi}$ in Ref. (14) has the following form:

$$
\begin{aligned}
\hat{D}_{\Phi} &= \hat{\Phi}(\alpha_1^+, \alpha_2^+) - \hat{\Phi}(\alpha_1^-, \alpha_2^-) \\
&= \begin{pmatrix}
0 & 0 & 0 & 0 & 0 & 0 & 0 & 0 & 0 \\
0 & e^{-i\alpha_r^+} - e^{-i\alpha_r^-} & 0 & 0 & 0 & 0 & 0 & 0 & 0 \\
0 & 0 & e^{i\alpha_r^+} - e^{i\alpha_r^-} & 0 & 0 & 0 & 0 & 0 & 0 \\
0 & 0 & 0 & 0 & 0 & 0 & 0 & 0 & 0 \\
0 & 0 & 0 & 0 & e^{-i\alpha_1^+} - e^{-i\alpha_1^-} & 0 & 0 & 0 & 0 \\
0 & 0 & 0 & 0 & 0 & e^{i\alpha_1^+} - e^{i\alpha_1^-} & 0 & 0 & 0 \\
0 & 0 & 0 & 0 & 0 & 0 & e^{-i\alpha_2^+} - e^{-i\alpha_2^-} & 0 & 0 \\
0 & 0 & 0 & 0 & 0 & 0 & 0 & e^{i\alpha_2^+} - e^{i\alpha_2^-} & 0 \\
0 & 0 & 0 & 0 & 0 & 0 & 0 & 0 & 0
\end{pmatrix}.
\end{aligned}
\tag{15}
$$

Here we introduce the notation for the relative phase of the bichromatic field:

$$
\alpha_r^+ = (\alpha_1^+ - \alpha_2^+), \quad \alpha_r^- = (\alpha_1^- - \alpha_2^-).
\tag{16}
$$

In accordance with Eqs. (11) and (15), we obtain the following expression for the matrix product $\hat{D}_{\Phi}\hat{G}_T$:

$$
\hat{D}_{\Phi}\hat{G}_T = e^{-\Gamma T}\hat{\Upsilon}_T,
\tag{17}
$$

where the matrix $\hat{\Upsilon}_T$ has the form

$$
\hat{\Upsilon}_T = \begin{pmatrix}
0 & 0 & 0 & 0 & 0 & 0 & 0 & 0 & 0 \\
0 & 0 & e^{-i\delta_{\mathrm{R}}T}(e^{-i\alpha_r^+} - e^{-i\alpha_r^-}) & 0 & 0 & 0 & 0 & 0 & 0 \\
0 & 0 & 0 & e^{i\delta_{\mathrm{R}}T}(e^{i\alpha_r^+} - e^{i\alpha_r^-}) & 0 & 0 & 0 & 0 & 0 \\
0 & 0 & 0 & 0 & 0 & 0 & 0 & 0 & 0 \\
0 & 0 & 0 & 0 & 0 & 0 & 0 & 0 & 0 \\
0 & 0 & 0 & 0 & 0 & 0 & 0 & 0 & 0 \\
0 & 0 & 0 & 0 & 0 & 0 & 0 & 0 & 0 \\
0 & 0 & 0 & 0 & 0 & 0 & 0 & 0 & 0 \\
0 & 0 & 0 & 0 & 0 & 0 & 0 & 0 & 0
\end{pmatrix}.
\tag{18}
$$

Then, taking into account Eq. (17), the error signal (14) is calculated by the formula

$$
S_{\mathrm{err}}(\delta_{\mathrm{R}}) = e^{-\Gamma T} \int_{t_2}^{t_2+\tau_{\mathrm{d}}} (\vec{\Omega}(t), \hat{W}_{\mathrm{d}}(t)\hat{\Upsilon}_T\hat{W}_{\mathrm{p}}\vec{\rho}_{\mathrm{in}})dt.
\tag{19}
$$

Thus, as it can be seen from Eq. (18), the error signal is sensitive only to a variation of the relative phase $\alpha_r = \alpha_1 - \alpha_2$, but does not depend on the phases $\alpha_{1,2}$ individually. Also note that the maximum amplitude of the error
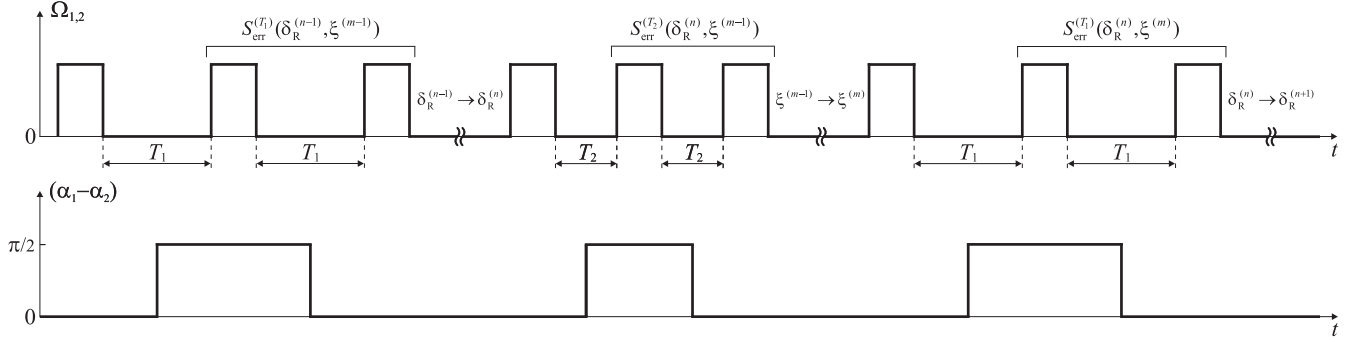
FIG. 3. Scheme of the GABRS-CPT sequence, where n and m are the step indices for the first and second servo loops, respectively.

signal (19) is achieved for the phase jumps $\alpha_r^+ = \pi/2$ and $\alpha_r^- = -\pi/2$.

In atomic clocks, the local oscillator frequency is stabilized at the zero of the error signal for the central Ramsey resonance. Therefore, one of the key parameters influencing the metrological characteristics is the frequency shift $\bar{\delta}_{\text{clock}}$, which corresponds to the solution of the equation

$$S_{\text{err}}(\delta_{\text{R}}) = 0, \tag{20}$$

in relation to δ_{R}.

III. GENERALIZED AUTOBALANCED RAMSEY SPECTROSCOPY OF CPT RESONANCES

The method of generalized autobalance Ramsey spectroscopy (GABRS) for optical frequency standards was developed within the framework of the two-level atomic model in Ref. [30]. Below we prove the applicability of this method for atomic clocks based on CPT resonances.

The stabilization scheme comprises two servo loops acting in parallel on alternately operated Ramsey sequences with the different free evolution times T_1 and T_2 (see Fig. 3). The first loop controls the Raman detuning δ_{R} (i.e., LO frequency), and the second loop governs some concomitant parameter ξ associated with the first and/or second Ramsey pulse. The GABRS algorithm is organized as a series of the following cycles. For the Ramsey sequence with the free evolution time T_1, the concomitant parameter is fixed (that is, $\xi = \xi_{\text{fixed}}$), and the variable detuning δ_{R} is stabilized at the zero of the first error signal: $S_{\text{err}}^{(T_1)}(\delta_{\text{R}}, \xi_{\text{fixed}}) = 0$. The operation of this servo loop can be presented as the following recurrent sequence:

$$\delta_{\text{R}}^{(n)} = \delta_{\text{R}}^{(n-1)} + r S_{\text{err}}^{(T_1)}(\delta_{\text{R}}^{(n-1)}, \xi_{\text{fixed}}), \tag{21}$$

where r is a feedback coefficient for the frequency loop, and n is the step index for the first servo loop. Then, measurements are carried out for a sequence of Ramsey pulses with other free evolution time T_2, where the previously obtained frequency is fixed (i.e., $\delta_{\text{R}} = \delta_{\text{fixed}}$) and the concomitant parameter ξ is stabilized at the zero of the second error signal: $S_{\text{err}}^{(T_2)}(\delta_{\text{fixed}}, \xi) = 0$. The operation of this second servo loop can be presented as another recurrent sequence:

$$\xi^{(m)} = \xi^{(m-1)} + q S_{\text{err}}^{(T_2)}(\delta_{\text{fixed}}, \xi^{(m-1)}), \tag{22}$$

where q is a feedback coefficient for the ξ loop, and m is the step index for the second servo loop. Repeating these iterations, we finally stabilize both parameters $\delta_{\text{R}} = \bar{\delta}_{\text{clock}}$ and

$\xi = \bar{\xi}$, which correspond to the solution of the system of equations

$$S_{\text{err}}^{(T_1)}(\delta_{\text{R}}, \xi) = 0, \quad S_{\text{err}}^{(T_2)}(\delta_{\text{R}}, \xi) = 0, \tag{23}$$

in relation to the two variables δ_{R} and ξ. Substituting the expression for the error signal (19) into Eq. (23), we obtain the following system of equations:

$$\int_{t_2}^{t_2+\tau_d} (\vec{\Omega}(t), \hat{W}_{\text{d}}(t)\hat{\Upsilon}_{T_1}\hat{W}_{\text{p}}\bar{\rho}_{\text{in}})dt = 0,$$

$$\int_{t_2}^{t_2+\tau_d} (\vec{\Omega}(t), \hat{W}_{\text{d}}(t)\hat{\Upsilon}_{T_2}\hat{W}_{\text{p}}\bar{\rho}_{\text{in}})dt = 0. \tag{24}$$

The fastest convergence of iterations (21) and (22) to the solution of Eq. (24) is performed for the following feedback coefficients:

$$r = -\left[\partial_{\delta_{\text{R}}} S_{\text{err}}^{(T_1)}(\delta_{\text{R}}, \xi)\big|_{\delta_{\text{R}}=\bar{\delta}_{\text{clock}}, \xi=\bar{\xi}}\right]^{-1},$$

$$q = -\left[\partial_{\xi} S_{\text{err}}^{(T_2)}(\delta_{\text{R}}, \xi)\big|_{\delta_{\text{R}}=\bar{\delta}_{\text{clock}}, \xi=\bar{\xi}}\right]^{-1}, \tag{25}$$

where $\partial_{\delta_{\text{R}}} = \partial/\partial\delta_{\text{R}}$ and $\partial_{\xi} = \partial/\partial\xi$ are the differential operators. In practice, the optimal values r and q are determined experimentally.

Let us show that the system (24) always has the solution $\delta_{\text{R}} = 0$. As can be seen from Eq. (18), in the case of $\delta_{\text{R}} = 0$, the following equality for the matrices $\hat{\Upsilon}_{T_1}$ and $\hat{\Upsilon}_{T_2}$ takes place:

$$\hat{\Upsilon}_{T_1}(\delta_{\text{R}} = 0) = \hat{\Upsilon}_{T_2}(\delta_{\text{R}} = 0) = \hat{D}_{\Phi}. \tag{26}$$

In this case, the system of two Eqs. (24) is reduced to one equation on unknown ξ:

$$\int_{t_2}^{t_2+\tau_d} (\vec{\Omega}(t), \hat{W}_{\text{d}}(t)\hat{D}_{\Phi}\hat{W}_{\text{p}}\bar{\rho}_{\text{in}})dt = 0, \tag{27}$$

which always has a solution.

Thus, we have analytically shown that the choice of the appropriate value of the concomitant parameter ξ allows us to suppress the light shift of the clock frequency ($\bar{\delta}_{\text{clock}} = 0$) stabilized by the CPT resonance. We emphasize that this result does not depend on the characteristics of the Ramsey pulses (amplitude, shape, duration, and phase structure), relaxation constants, errors in the generation of phase jumps, etc. Such a resistance of this method to various technical imperfections determines its high reliability.

Note that the typical Ramsey signal consists of a large number of fringes [see Fig. 4(a)]. As a result, the system of
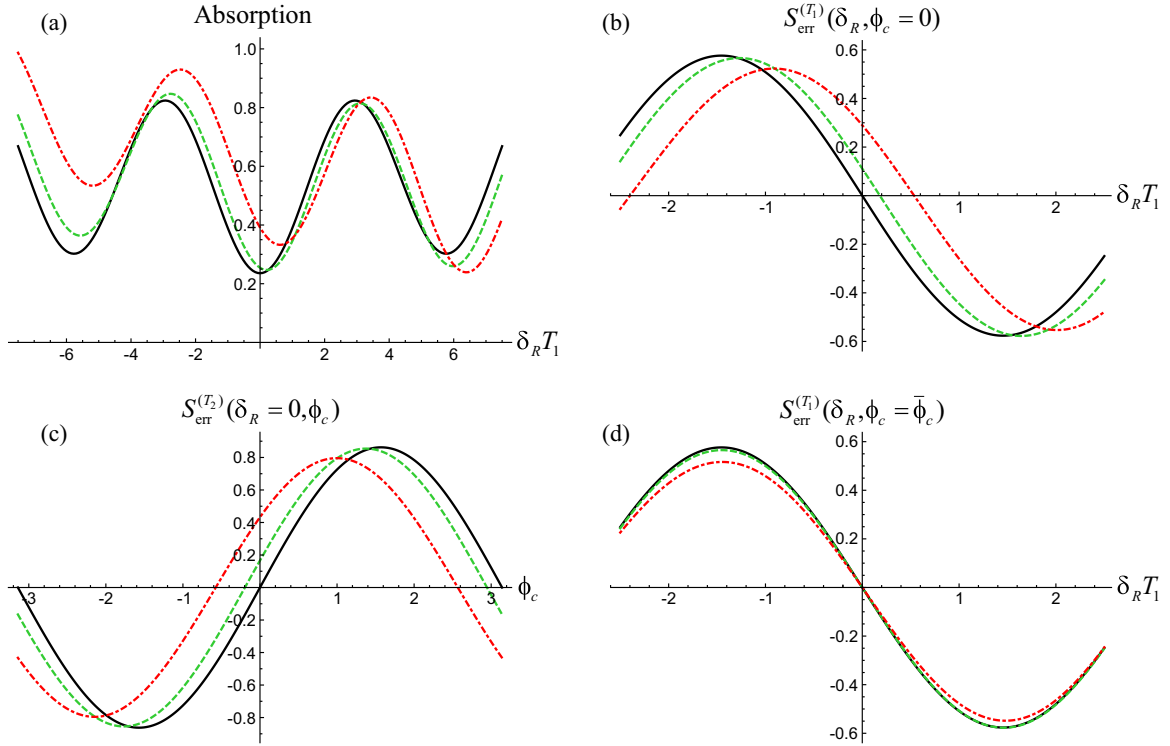
FIG. 4. (a) Ramsey-CPT fringes in the absorption signal (7). (b) Error signal $S_{\mathrm{err}}^{(T_1)}(\delta_{\mathrm{R}}, \phi_c = 0)$ in the standard Ramsey scheme. (c) Error signal $S_{\mathrm{err}}^{(T_2)}(\delta_{\mathrm{R}} = 0, \phi_c)$ for stabilization of the correction phase. (d) Error signal $S_{\mathrm{err}}^{(T_1)}(\delta_{\mathrm{R}}, \phi_c = \bar{\phi}_c)$ for stabilization of the LO frequencies in the autobalanced Ramsey scheme with the correction phase. The graphs are calculated for the following values of the light shift of the Raman transition: $\Delta_{\mathrm{sh}}/\gamma_{\mathrm{CPT}} = 0$ (black solid line), $\Delta_{\mathrm{sh}}/\gamma_{\mathrm{CPT}} = 0.1$ (green dashed line), and $\Delta_{\mathrm{sh}}/\gamma_{\mathrm{CPT}} = 0.3$ (red dot-and-dash line). Numerical parameters of the model are as follows: $\Omega_1 = \Omega_2 = 0.25\,\gamma_{\mathrm{sp}}$, $\gamma_1 = \gamma_2 = \gamma_{\mathrm{sp}}/2$, $\gamma_{\mathrm{opt}} = 50\,\gamma_{\mathrm{sp}}$, $\Gamma = 5 \times 10^{-5}\gamma_{\mathrm{sp}}$, $T_1 = 0.5\,\Gamma^{-1}$, $T_2 = 0.1\,\Gamma^{-1}$, $\tau_{\mathrm{p}} = \infty$ (steady state), $\tau_{\mathrm{d}} = 5\,\gamma_{\mathrm{CPT}}^{-1}$, and $\alpha_r^{\pm} = \pm\pi/2$.

Eqs. (24) has a series of the solutions

$$\delta_{\mathrm{R}} = n\pi/(T_1 - T_2) \quad (n = 0, \pm 1, \pm 2, \dots) \tag{28}$$

related not only to the central Ramsey resonance but also to other fringes (for $n \neq 0$). These solutions are determined by the condition

$$\hat{\Upsilon}_{T_1} = \pm\hat{\Upsilon}_{T_2} \quad \Rightarrow \quad e^{i\delta_{\mathrm{R}}T_1} = \pm e^{i\delta_{\mathrm{R}}T_2}. \tag{29}$$

In this case, the corresponding concomitant parameter $\bar{\xi}$ can be found from the equation

$$\int_{t_2}^{t_2+\tau_{\mathrm{d}}} (\vec{\Omega}(t), \hat{W}_{\mathrm{d}}(t)\hat{\Upsilon}_{T_2}\hat{W}_{\mathrm{p}}\vec{\rho}_{\mathrm{in}})dt = 0. \tag{30}$$

However, frequency stabilization in atomic clocks is carried out by the central Ramsey resonance ($\delta_{\mathrm{R}} = 0$). Therefore, the identification of the central fringe is an important technical problem, which has been considered in several works [38–41].

A. GABRS-CPT with a correction phase

As the first particular case of GABRS for CPT resonances, we consider the scheme where a concomitant stabilized parameter is the additional shift of the relative phase of the bichromatic field during the second Ramsey pulse, i.e., $\xi = \phi_c$. The correction phase, $\phi_c = \bar{\phi}_c$, for which the light shift of the stabilized frequency is absent ($\bar{\delta}_{\mathrm{clock}} = 0$), can be found from Eq. (27). A comparison of the usual Ramsey scheme

and the GABRS with the correction phase for different field-induced shifts Δ_{sh} of the clock transition is shown in Fig. 4. Hereinafter, for convenience we determine the frequencies in units of half-width at half-maximum of the steady-state CPT resonance γ_{CPT} (see, for example, Ref. [42]):

$$\gamma_{\mathrm{CPT}} \approx \left(\Gamma + \frac{\Omega_1^2 + \Omega_2^2}{\gamma_{\mathrm{opt}}}\right). \tag{31}$$

In the calculations, we assume that during the first Ramsey pulse the atoms are pumped into the steady state (i.e., formally $\tau_{\mathrm{p}} = \infty$), which corresponds, in practice, to the condition $\tau_{\mathrm{p}} \gg \gamma_{\mathrm{CPT}}^{-1}$. As follows from Eqs. (19) and (27), the duration and the shape of the pumping Ramsey pulse can only affect the value of the concomitant parameter $\bar{\xi}$ and the slope of the error signals, while the light-shift suppression ($\bar{\delta}_{\mathrm{clock}} = 0$) is independent of pulse parameters. Figure 4(d) demonstrates the efficiency of this GABRS scheme for suppressing the light shift of the error signal $S_{\mathrm{err}}^{(T_1)}(\delta_{\mathrm{R}}, \bar{\phi}_c)$, which is used to stabilize the LO frequency. The dependence of the correction phase $\bar{\phi}_c$ on the detection (accumulation) time of the spectroscopic signal τ_{d} is shown in Fig. 5(a). In Fig. 5(b), the dependence of the correction phase $\bar{\phi}_c$ on the frequency shift of the clock transition Δ_{sh} is presented. Under the condition $\tau_{\mathrm{d}} \gg \gamma_{\mathrm{CPT}}^{-1}$, this dependence is well described by the formula:

$$\bar{\phi}_c(\Delta_{\mathrm{sh}}) \approx -2\arctan(\Delta_{\mathrm{sh}}/\gamma_{\mathrm{CPT}}). \tag{32}$$
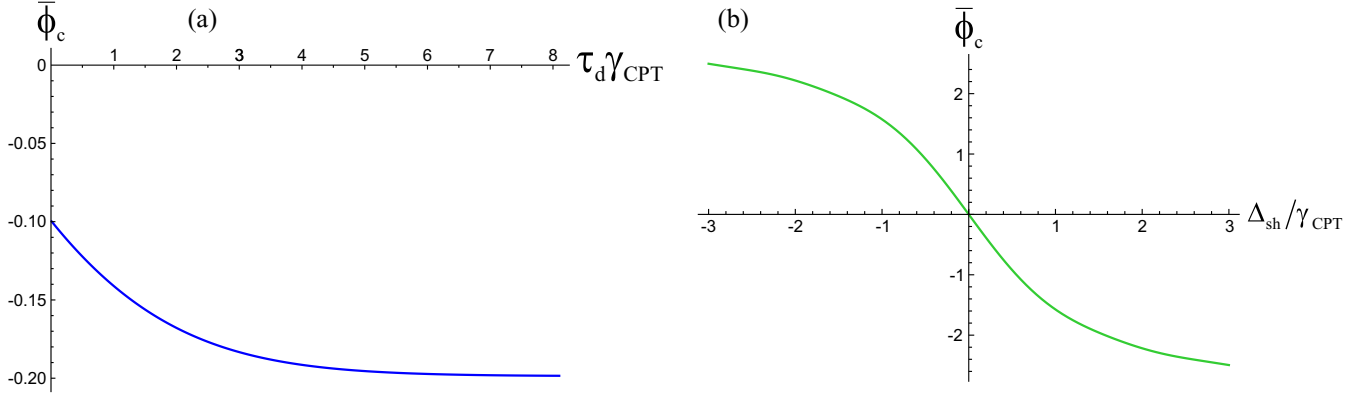
FIG. 5. (a) Dependence of the correction phase $\bar{\phi}_c$ on the detection time τ_d at $\Delta_{sh}/\gamma_{CPT} = 0.1$. (b) Dependence of the correction phase $\bar{\phi}_c$ on the frequency shift of the clock transition Δ_{sh} at $\tau_d = 5\,\gamma_{CPT}^{-1}$. Numerical parameters of the model: $\Omega_1 = \Omega_2 = 0.25\,\gamma_{sp}$, $\gamma_1 = \gamma_2 = \gamma_{sp}/2$, $\gamma_{opt} = 50\,\gamma_{sp}$, $\Gamma = 5 \times 10^{-5}\,\gamma_{sp}$, $T_1 = 0.5\,\Gamma^{-1}$, $T_2 = 0.1\,\Gamma^{-1}$, $\tau_p = \infty$ (steady state), and $\alpha_r^\pm = \pm\pi/2$.

B. GABRS-CPT with compensating frequency jumps

As the second particular case of GABRS for CPT resonances, we consider the scheme where a concomitant stabilized parameter is an additional jump in the frequency difference $(\omega_1 - \omega_2)$ during both Ramsey pulses, i.e., $\xi = \Delta_c$. The frequency jump ($\Delta_c = \bar{\Delta}_c$), which completely compensates the light shift ($\bar{\delta}_{clock} = 0$), can be found from Eq. (27). In Fig. 6(a) the error signals for the standard Ramsey scheme under different values of light shift Δ_{sh} are shown. Graphs of the error signals for stabiliza-

tion of the concomitant parameter Δ_c are presented in Fig. 6(b). Figure 6(c) demonstrates the error signals for frequency stabilization when $\Delta_c = \bar{\Delta}_c$. In contrast to the GABRS with correction phase, here the error signals $S_{err}^{(T_1)}(\delta_R, \Delta_c = \bar{\Delta}_c)$ for different values of Δ_{sh} completely coincide and have an antisymmetric shape. Also note that the value of the stabilized concomitant parameter $\bar{\Delta}_c$ does not depend on the detection time τ_d. The dependence of the frequency jump $\bar{\Delta}_c$ on the light shift Δ_{sh} has obviously linear form: $\bar{\Delta}_c = \Delta_{sh}$ [see Fig. 6(d)].
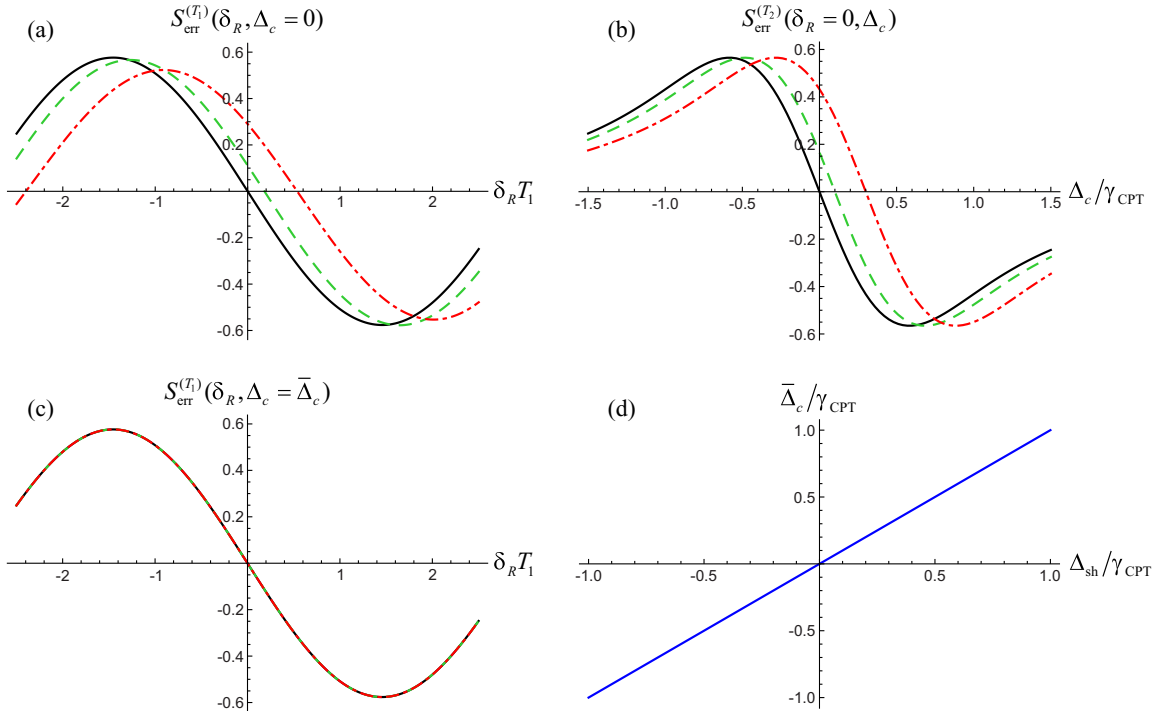

FIG. 6. (a) Error signal $S_{err}^{(T_1)}(\delta_R, \Delta_c = 0)$ in the standard Ramsey scheme. (b) Error signal $S_{err}^{(T_2)}(\delta_R = 0, \Delta_c)$ for stabilization of the additional frequency jump. (c) Error signal $S_{err}^{(T_1)}(\delta_R, \Delta_c = \bar{\Delta}_c)$ for stabilization of the LO frequencies in the autobalanced Ramsey scheme with the additional frequency jump. (d) Dependence of the frequency jump $\bar{\Delta}_c$ on the frequency shift of the clock transition Δ_{sh}. The graphs (a)–(c) are calculated for the following values of the light shift of the Raman transition: $\Delta_{sh}/\gamma_{CPT} = 0$ (black solid line), $\Delta_{sh}/\gamma_{CPT} = 0.1$ (green dashed line), and $\Delta_{sh}/\gamma_{CPT} = 0.3$ (red dot-and-dash line). Numerical parameters of the model are as follows: $\Omega_1 = \Omega_2 = 0.25\,\gamma_{sp}$, $\gamma_1 = \gamma_2 = \gamma_{sp}/2$, $\gamma_{opt} = 50\,\gamma_{sp}$, $\Gamma = 5 \times 10^{-5}\,\gamma_{sp}$, $T_1 = 0.5\,\Gamma^{-1}$, $T_2 = 0.1\,\Gamma^{-1}$, $\tau_p = \infty$ (steady state), $\tau_d = 5\,\gamma_{CPT}^{-1}$, and $\alpha_r^\pm = \pm\pi/2$.

In theory, both considered variants of the GABBS lead to the same result, which consists in complete suppression of the light shift. However, in practice the efficiency of these methods may be different. Therefore, the experimental comparison of these two schemes during the measurement of the Allan deviation has a great interest.

IV. COMBINED ERROR SIGNAL IN RAMSEY SPECTROSCOPY OF CPT RESONANCES

The protocol of the combined error signal in Ramsey spectroscopy (CESRS) of clock transitions was proposed in Ref. [31]. Below, we rigorously prove the applicability of this method for CPT resonances in the framework of the three-level Λ model.

This approach is also based on the excitation and interrogation of atoms using two sequences of Ramsey pulses with different free evolution times T_1 and T_2. However, in contrast to the GABRS, only one feedback loop is employed here. In this case, the error signal for the frequency stabilization is formed as a linear superposition of two usual error signals obtained separately for each Ramsey sequence:

$$S_{\text{err}}^{(\text{CES})}(\delta_{\text{R}}) = S_{\text{err}}^{(T_1)}(\delta_{\text{R}}) - \beta_{\text{cal}} S_{\text{err}}^{(T_2)}(\delta_{\text{R}}), \qquad (33)$$

where β_{cal} is some calibration coefficient. The stabilized frequency of the local oscillator corresponds to the condition when the combined error signal is zero: $S_{\text{err}}^{(\text{CES})}(\delta_{\text{R}}) = 0$. Substituting the expression (19) in the formula (33), we obtain

$$S_{\text{err}}^{(\text{CES})}(\delta_{\text{R}}) = e^{-\Gamma T_1} \left[\int_{t_2}^{t_2+\tau_{\text{d}}} (\vec{\Omega}(t), \hat{W}_{\text{d}}(t)\hat{\Upsilon}_{T_1}\hat{W}_{\text{p}}\vec{\rho}_{\text{in}})dt \right.$$
$$\left. - \beta_{\text{cal}} e^{\Gamma(T_1-T_2)} \int_{t_2}^{t_2+\tau_{\text{d}}} (\vec{\Omega}(t), \hat{W}_{\text{d}}(t)\hat{\Upsilon}_{T_2}\hat{W}_{\text{p}}\vec{\rho}_{\text{in}})dt \right]. \qquad (34)$$

Setting the calibration coefficient equal to

$$\beta_{\text{cal}} = e^{-\Gamma(T_1-T_2)}, \qquad (35)$$

we can write the expression for the combined error signal (34) as follows

$$S_{\text{err}}^{(\text{CES})}(\delta_{\text{R}}) = e^{-\Gamma T_1} \int_{t_2}^{t_2+\tau_{\text{d}}} (\vec{\Omega}(t), \hat{W}_{\text{d}}(t)(\hat{\Upsilon}_{T_1} - \hat{\Upsilon}_{T_2})\hat{W}_{\text{p}}\vec{\rho}_{\text{in}})dt. \qquad (36)$$

Taking into account the equality (26) for the matrices $\hat{\Upsilon}_{T_1}$ and $\hat{\Upsilon}_{T_2}$ at $\delta_{\text{R}} = 0$, from Eq. (36) we find

$$S_{\text{err}}^{(\text{CES})}(0) = 0. \qquad (37)$$

Thus, the performed analysis proves the absence of the light shift for the LO frequency stabilized at zero of the combined error signal (33) with the calibration coefficient (35).

Figure 7 shows the error signals for the standard Ramsey scheme under two different times of the free evolution ($T_1/T_2 = 10$) and the combined error signal. It can be seen that for the accurate calibration coefficient β_{cal}, the light shift for CESRS is completely suppressed. However, under real conditions, β_{cal} may differ from the ideal value, which leads to the appearance of a residual shift for the combined error signal. Nevertheless, as calculations show (see Fig. 8), even $\pm 5\%$ deviation of β_{cal} from the ideal value provides
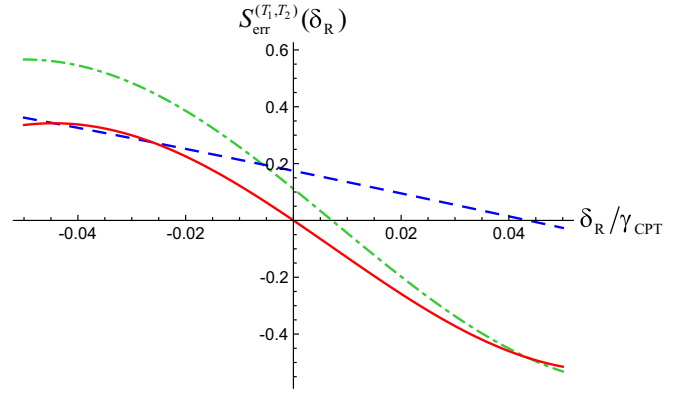

FIG. 7. Error signals: The green dot-and-dash line corresponds to the usual Ramsey scheme for $T = 0.5\,\Gamma^{-1}$, the blue dashed line corresponds to the usual Ramsey scheme for $T = 0.05\,\Gamma^{-1}$, and red solid line corresponds to the combined error signal for $T_1 = 0.5\,\Gamma^{-1}$ and $T_2 = 0.05\,\Gamma^{-1}$. Numerical parameters of the model are as follows: $\Delta_{\text{sh}}/\gamma_{\text{CPT}} = 0.1$, $\Omega_1 = \Omega_2 = 0.25\,\gamma_{\text{sp}}$, $\gamma_1 = \gamma_2 = \gamma_{\text{sp}}/2$, $\gamma_{\text{opt}} = 50\,\gamma_{\text{sp}}$, $\Gamma = 5 \times 10^{-5}\,\gamma_{\text{sp}}$, $\tau_{\text{p}} = \infty$ (steady state), $\tau_{\text{d}} = 5\,\gamma_{\text{CPT}}^{-1}$, and $\alpha_r^{\pm} = \pm\pi/2$.

suppression of the light shift for the CESRS protocol about 15 times that compared with the usual Ramsey scheme (with the free evolution time T_1).

The modified variant of the combined error signal in Ramsey spectroscopy (MCESRS) for CPT resonances is considered in Appendix B. This method allows us to integrate two successive interrogations of atoms under different times of free evolution in one cycle. A potential advantage of MCESRS compared to CESRS is a decrease by about 2 times the duration of one cycle required to correct the stabilized frequency.
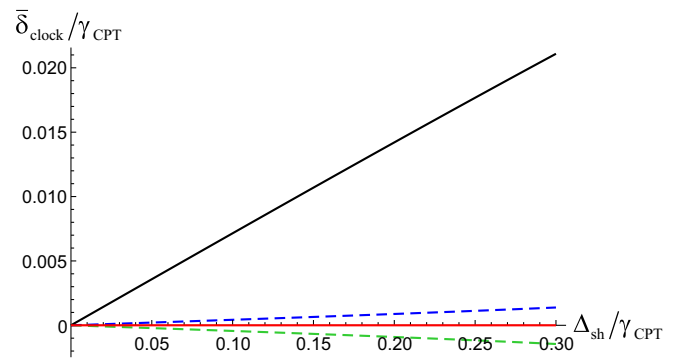

FIG. 8. Shift of the clock frequency $\bar{\delta}_{\text{clock}}$ versus the light shift Δ_{sh}. The black solid line is calculated for the usual Ramsey scheme ($T = 0.5\,\Gamma^{-1}$), the red solid line is calculated for the CESRS ($T_1 = 0.5\,\Gamma^{-1}$ and $T_2 = 0.05\,\Gamma^{-1}$) in the case of the ideal value (35) of the calibration coefficient β_{cal}, the green dashed line is calculated for the CESRS if β_{cal} deviates by $+5\%$ from the ideal value, and the blue dashed line is calculated for the CESRS if β_{cal} deviates by -5% from the ideal value. Numerical parameters of the model are as follows: $\Omega_1 = \Omega_2 = 0.25\,\gamma_{\text{sp}}$, $\gamma_1 = \gamma_2 = \gamma_{\text{sp}}/2$, $\gamma_{\text{opt}} = 50\,\gamma_{\text{sp}}$, $\Gamma = 5 \times 10^{-5}\,\gamma_{\text{sp}}$, $\tau_{\text{p}} = \infty$ (steady state), $\tau_{\text{d}} = 5\,\gamma_{\text{CPT}}^{-1}$, and $\alpha_r^{\pm} = \pm\pi/2$.

V. CONCLUSION

The applicability of the methods of generalized autobalanced Ramsey spectroscopy (GABRS) and the combined error signal in Ramsey spectroscopy (CESRS) for resonances of coherent population trapping (CPT) is rigorously proved. The analytical results are confirmed by numerical calculations demonstrating the high efficiency of suppressing light shift and its fluctuations. For GABRS, two variants of a concomitant parameter are considered in detail. In the first case, the additional variation of the relative phase for the second Ramsey pulse of the bichromatic field is used. In the second case, it is proposed to introduce during the Ramsey pulses the additional shift in the Raman detuning for compensation of the light shift. In addition, a modified version of CESRS is considered, in which two successive interrogations with different times of free evolution are combined in one cycle. The implementation of the GABRS and CESRS methods can significantly improve the long-term stability and accuracy of CPT atomic clocks. An advantage of the these spectroscopic schemes is also their high immunity to various distortions of the pulse shape, relaxation processes, errors in the formation of phase jumps, etc.

APPENDIX A

The Liouvillian $\hat{L}$ is determined by Eqs. (3)–(5):

$$
\hat{L} = \begin{pmatrix}
-\Gamma/2 & 0 & 0 & \Gamma/2 & -i\Omega_1 & i\Omega_1^* & 0 & 0 & \gamma_1 + \Gamma/2 \\
0 & -\Gamma - i(\delta_R - \Delta_{sh}) & 0 & 0 & -i\Omega_2 & 0 & 0 & i\Omega_1^* & 0 \\
0 & 0 & -\Gamma + i(\delta_R - \Delta_{sh}) & 0 & 0 & i\Omega_2^* & -i\Omega_1 & 0 & 0 \\
\Gamma/2 & 0 & 0 & -\Gamma/2 & 0 & 0 & -i\Omega_2 & i\Omega_2^* & \gamma_2 + \Gamma/2 \\
-i\Omega_1^* & -i\Omega_2^* & 0 & 0 & -\gamma_{opt} - i\delta_1 & 0 & 0 & 0 & i\Omega_1^* \\
i\Omega_1 & 0 & i\Omega_2 & 0 & 0 & -\gamma_{opt} + i\delta_1 & 0 & 0 & -i\Omega_1 \\
0 & 0 & -i\Omega_1^* & -i\Omega_2^* & 0 & 0 & -\gamma_{opt} - i\delta_2 & 0 & i\Omega_2^* \\
0 & i\Omega_1 & 0 & i\Omega_2 & 0 & 0 & 0 & -\gamma_{opt} + i\delta_2 & -i\Omega_2 \\
0 & 0 & 0 & 0 & i\Omega_1 & -i\Omega_1^* & i\Omega_2 & -i\Omega_2^* & -\gamma_{sp} - \Gamma
\end{pmatrix}. \tag{A1}
$$

In the absence of the light field ($\Omega_1 = \Omega_2 = 0$ and $\Delta_{sh} = 0$), the Liouvillian $\hat{L}$ takes the following form:

$$
\hat{L}_0 = \begin{pmatrix}
-\Gamma/2 & 0 & 0 & \Gamma/2 & 0 & 0 & 0 & 0 & \gamma_1 + \Gamma/2 \\
0 & -\Gamma - i\delta_R & 0 & 0 & 0 & 0 & 0 & 0 & 0 \\
0 & 0 & -\Gamma + i\delta_R & 0 & 0 & 0 & 0 & 0 & 0 \\
\Gamma/2 & 0 & 0 & -\Gamma/2 & 0 & 0 & 0 & 0 & \gamma_2 + \Gamma/2 \\
0 & 0 & 0 & 0 & -\gamma_{opt} - i\delta_1 & 0 & 0 & 0 & 0 \\
0 & 0 & 0 & 0 & 0 & -\gamma_{opt} + i\delta_1 & 0 & 0 & 0 \\
0 & 0 & 0 & 0 & 0 & 0 & -\gamma_{opt} - i\delta_2 & 0 & 0 \\
0 & 0 & 0 & 0 & 0 & 0 & 0 & -\gamma_{opt} + i\delta_2 & 0 \\
0 & 0 & 0 & 0 & 0 & 0 & 0 & 0 & -\gamma_{sp} - \Gamma
\end{pmatrix}. \tag{A2}
$$

The operator $\hat{G}_T = e^{\hat{L}_0 T}$ describes the free evolution of atoms:

$$
\hat{G}_T = \begin{pmatrix}
G_{11} & 0 & 0 & G_{14} & 0 & 0 & 0 & 0 & G_{19} \\
0 & e^{-(\Gamma+i\delta_R)T} & 0 & 0 & 0 & 0 & 0 & 0 & 0 \\
0 & 0 & e^{-(\Gamma-i\delta_R)T} & 0 & 0 & 0 & 0 & 0 & 0 \\
G_{41} & 0 & 0 & G_{44} & 0 & 0 & 0 & 0 & G_{49} \\
0 & 0 & 0 & 0 & e^{-(\gamma_{\mathrm{opt}}+i\delta_1)T} & 0 & 0 & 0 & 0 \\
0 & 0 & 0 & 0 & 0 & e^{-(\gamma_{\mathrm{opt}}-i\delta_1)T} & 0 & 0 & 0 \\
0 & 0 & 0 & 0 & 0 & 0 & e^{-(\gamma_{\mathrm{opt}}+i\delta_2)T} & 0 & 0 \\
0 & 0 & 0 & 0 & 0 & 0 & 0 & e^{-(\gamma_{\mathrm{opt}}-i\delta_2)T} & 0 \\
0 & 0 & 0 & 0 & 0 & 0 & 0 & 0 & e^{-(\gamma_{\mathrm{sp}}+\Gamma)T}
\end{pmatrix}, \quad \text{(A3)}
$$

where

$$
G_{11} = G_{44} = \tfrac{1}{2}(1 + e^{-\Gamma T}), \tag{A4}
$$

$$
G_{14} = G_{41} = \tfrac{1}{2}(1 - e^{-\Gamma T}), \tag{A5}
$$

$$
G_{19} = \frac{\gamma_1 + \gamma_2 + \Gamma}{2(\gamma_{\mathrm{sp}} + \Gamma)} + \frac{\gamma_1 - \gamma_2}{2\gamma_{\mathrm{sp}}} e^{-\Gamma T}
$$
$$
- \frac{\gamma_{\mathrm{sp}}(2\gamma_1 + \Gamma) + \Gamma(\gamma_1 - \gamma_2)}{2\gamma_{\mathrm{sp}}(\gamma_{\mathrm{sp}} + \Gamma)} e^{-(\gamma_{\mathrm{sp}}+\Gamma)T}, \tag{A6}
$$

$$
G_{49} = \frac{\gamma_1 + \gamma_2 + \Gamma}{2(\gamma_{\mathrm{sp}} + \Gamma)} - \frac{\gamma_1 - \gamma_2}{2\gamma_{\mathrm{sp}}} e^{-\Gamma T}
$$
$$
- \frac{\gamma_{\mathrm{sp}}(2\gamma_2 + \Gamma) - \Gamma(\gamma_1 - \gamma_2)}{2\gamma_{\mathrm{sp}}(\gamma_{\mathrm{sp}} + \Gamma)} e^{-(\gamma_{\mathrm{sp}}+\Gamma)T}. \tag{A7}
$$

APPENDIX B: MODIFIED CESRS-CPT

In this section, we discuss two variants of a modified combined error signal in Ramsey spectroscopy (MCESRS) of the coherent-population-trapping (CPT) resonances. The main idea of this spectroscopic scheme is to join two Ramsey cycles with different free evolution times in one cycle. This can be

achieved by using a Ramsey sequence, which consists of three pulses separated by time intervals with different durations T_S and T_L, as shown in Fig. 9. The first pulse must be long enough to pump the atoms into a dark state. Two subsequent short pulses interrogate the atoms. The duration of the first detecting pulse should be short enough so as not to destroy the atomic
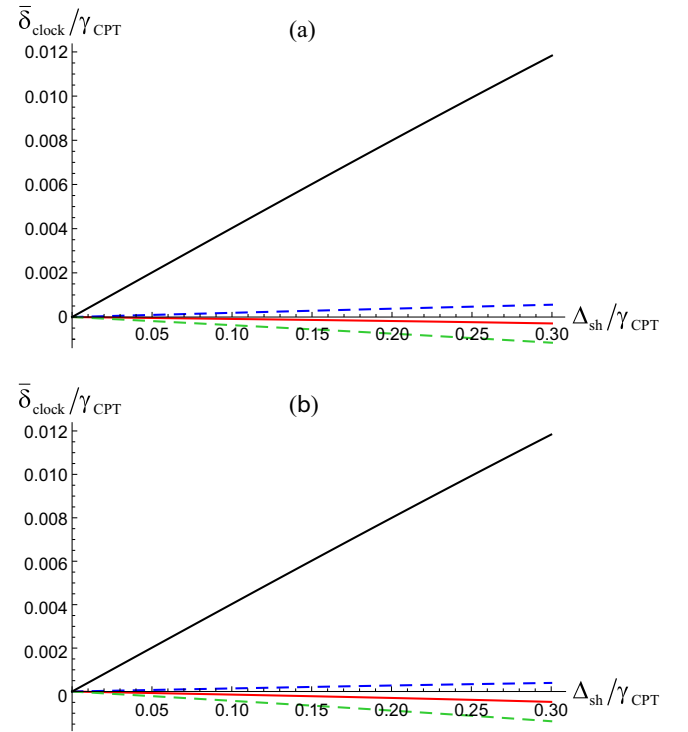
FIG. 10. Shift of the clock frequency $\bar{\delta}_{\mathrm{clock}}$ versus the light shift Δ_{sh} for MCESRS: (a) detecting pulses of the equal durations; (b) detecting pulses of the different durations. The black solid line is calculated for the usual Ramsey scheme ($T = 0.5\,\Gamma^{-1}$), the red solid line is calculated for the MCESRS ($T_L = 0.5\,\Gamma^{-1}$ and $T_S = 0.05\,\Gamma^{-1}$) in the case of the ideal value (B2) of the calibration coefficient β_{cal}, the green dashed line is calculated for the MCESRS if β_{cal} deviates by $+5\%$ from the ideal value, and the blue dashed line is calculated for the MCESRS if β_{cal} deviates by -5% from the ideal value. Numerical parameters of the model are as follows: $\Omega_1 = \Omega_2 = 0.25\,\gamma_{\mathrm{sp}}$, $\gamma_1 = \gamma_2 = \gamma_{\mathrm{sp}}/2$, $\gamma_{\mathrm{opt}} = 50\,\gamma_{\mathrm{sp}}$, $\Gamma = 5 \times 10^{-5}\,\gamma_{\mathrm{sp}}$, $\tau_{\mathrm{p}} = \infty$ (steady state), $\tau_{\mathrm{d}} = \tau_S = 0.15\,\gamma_{\mathrm{CPT}}^{-1}$, and $\alpha_r^{\pm} = \pm\pi/2$.
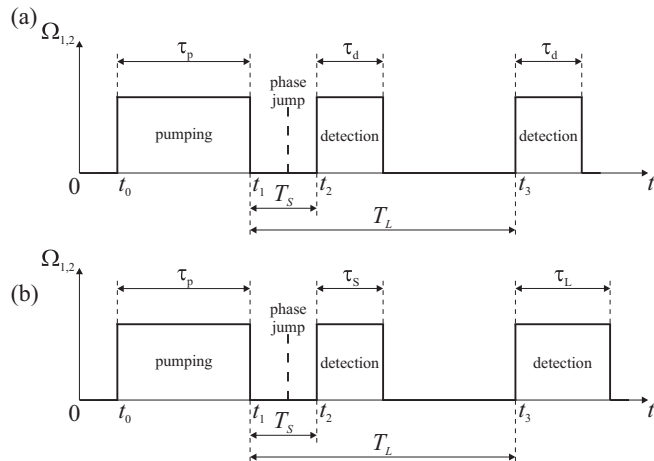
FIG. 9. Scheme of a three-pulse Ramsey-type sequence. The first pulse pumps atoms into a dark state. Two subsequent pulses detect the spectroscopic information.

coherence. A spectroscopic signal (for example, absorption or transmission) is recorded for each detecting pulse, after which the combined error signal is calculated as a superposition of the usual error signals.

In the first version of the MCESRS, we propose to use detecting pulses of equal durations [see Fig. 9(a)]. The combined error signal has the form

$$S_{\text{err}}^{(\text{MCES-1})}(\delta_{\text{R}}) = S_{\text{err}}^{(T_L)}(\delta_{\text{R}}) - \beta_{\text{cal}}^{(\text{MCES})} S_{\text{err}}^{(T_S)}(\delta_{\text{R}}), \quad \text{(B1)}$$

where the calibration coefficient according to Eq. (35) is

$$\beta_{\text{cal}}^{(\text{MCES})} = e^{-\Gamma(T_L - T_S)}. \quad \text{(B2)}$$

In the second version of the MCESRS, it is proposed to use detecting pulses of different durations [see Fig. 9(b)]. This scheme is based on the fact that the amplitude of the error signal is proportional to the duration of the detecting pulses if $\tau_S, \tau_L \ll \gamma_{\text{CPT}}^{-1}$. In this case, the error signal is calculated as

follows:

$$S_{\text{err}}^{(\text{MCES-2})}(\delta_{\text{R}}) = S_{\text{err}}^{(T_L)}(\delta_{\text{R}}) - S_{\text{err}}^{(T_S)}(\delta_{\text{R}}), \quad \text{(B3)}$$

where the ratio between the pulse durations is determined by the calibration coefficient (B2):

$$\frac{\tau_S}{\tau_L} = \beta_{\text{cal}}^{(\text{MCES})}, \quad \text{(B4)}$$

where τ_S and τ_L are the durations of the first and second interrogating pulses, respectively.

Phase jumps must be performed before the first detecting pulse. Figure 10 demonstrates a comparison of the standard Ramsey scheme and two variants of the MCESRS (see Fig. 9). From these graphs it can be seen that even for $\pm 5\%$ deviations of the calibration coefficient (B2) the proposed methods provide a significant suppression of the light shift.

Note that the MCESRS technique is specific for CPT clocks and not applicable for optical atomic clocks.

[1] F. Riehle, *Frequency Standards: Basics and Applications* (Wiley-VCH, New York, 2005).

[2] J. Vanier and C. Tomescu, *The Quantum Physics of Atomic Frequency Standards* (CRC, Boca Raton, FL, 2015).

[3] A. D. Ludlow, M. M. Boyd, J. Ye, E. Peik, and P. O. Schmidt, Optical atomic clocks, Rev. Mod. Phys. **87**, 637 (2015).

[4] A. Godone, F. Levi, C. E. Calosso, and S. Micalizio, High-performing vapor-cell frequency standards, Riv. Nuovo Cim. **38**, 133 (2015).

[5] M. Kajita, *Measuring Time: Frequency Measurements and Related Developments in Physics* (Institute of Physics, Bristol, England, 2018).

[6] L. Maleki and J. Prestage, Applications of clocks and frequency standards: From the routine to tests of fundamental models, Metrologia **42**, S145 (2005).

[7] J. D. Prestage and G. L. Weaver, Atomic clocks and oscillators for deep-space navigation and radio science, Proc. IEEE **95**, 2235 (2007).

[8] A. Derevianko and M. Pospelov, Hunting for topological dark matter with atomic clocks, Nat. Phys. **10**, 933 (2014).

[9] C. Lisdat, G. Grosche, N. Quintin *et al.*, A clock network for geodesy and fundamental science, Nat. Commun. **7**, 12443 (2016).

[10] Y. Bock and D. Melgar, Physical applications of GPS geodesy: A review, Rep. Prog. **79**, 106801 (2016).

[11] T. E. Mehlstäubler, G. Grosche, Chr. Lisdat, P. O. Schmidt, and H. Denker, Atomic clocks for geodesy, Rep. Prog. **81**, 064401 (2018).

[12] G. Alzetta, A. Gozzini, M. Moi, and G. Orriols, An experimental method for the observation of r.f. transitions and laser beat resonances in oriented Na vapour, Nuovo Cimento B **36**, 5 (1976).

[13] B. D. Agap'ev, M. B. Gornyi, B. G. Matisov, and Y. V. Rozhdestvenskii, Coherent population trapping in quantum systems, Phys.-Usp. **36**, 763 (1993).

[14] E. Arimondo, Coherent population trapping in laser spectroscopy, Prog. Opt. **35**, 257 (1996).

[15] J. Vanier, Atomic clocks based on coherent population trapping: A review, Appl. Phys. B **81**, 421 (2005).

[16] V. Shah and J. Kitching, Advances in coherent population trapping for atomic clocks, Adv. At., Mol., Opt. Phys. **59**, 21 (2010).

[17] S. Knappe, P. D. D. Schwindt, V. Shah, L. Hollberg, J. Kitching, L. Liew, and J. Moreland, A chip-scale atomic clock based on ^{87}Rb with improved frequency stability, Opt. Express **13**, 1249 (2005).

[18] Z. Wang, Review of chip-scale atomic clocks based on coherent population trapping, Chin. Phys. B **23**, 030601 (2014).

[19] J. Kitching, Chip-scale atomic devices, Appl. Phys. Rev. **5**, 031302 (2018).

[20] N. F. Ramsey, A molecular beam resonance method with separated oscillating fields, Phys. Rev. **78**, 695 (1950).

[21] V. I. Yudin, A. V. Taichenachev, C. W. Oates, Z. W. Barber, N. D. Lemke, A. D. Ludlow, U. Sterr, C. Lisdat, and F. Riehle, Hyper-Ramsey spectroscopy of optical clock transitions, Phys. Rev. A **82**, 011804(R) (2010).

[22] N. Huntemann, B. Lipphardt, M. Okhapkin, C. Tamm, E. Peik, A. V. Taichenachev, and V. I. Yudin, Generalized Ramsey Excitation Scheme with Suppressed Light Shift, Phys. Rev. Lett. **109**, 213002 (2012).

[23] N. Huntemann, C. Sanner, B. Lipphardt, Chr. Tamm, and E. Peik, Single-Ion Atomic Clock with 3×10^{-18} Systematic Uncertainty, Phys. Rev. Lett. **116**, 063001 (2016).

[24] R. Hobson, W. Bowden, S. A. King, P. E. G. Baird, I. R. Hill, and P. Gill, Modified hyper-Ramsey methods for the elimination of probe shifts in optical clocks, Phys. Rev. A **93**, 010501(R) (2016).

[25] T. Zanon-Willette, V. I. Yudin, and A. V. Taichenachev, Generalized hyper-Ramsey resonance with separated oscillating fields, Phys. Rev. A **92**, 023416 (2015).

[26] T. Zanon-Willette, E. de Clercq, and E. Arimondo, Probe light-shift elimination in generalized hyper-Ramsey quantum clocks, Phys. Rev. A **93**, 042506 (2016).

[27] V. I. Yudin, A. V. Taichenachev, M. Yu. Basalaev, and T. Zanon-Willette, Synthetic frequency protocol for Ramsey spectroscopy of clock transitions, Phys. Rev. A **94**, 052505 (2016).

[28] T. Zanon-Willette, R. Lefevre, R. Metzdorff, N. Sillitoe, S. Almonacil, M. Minissale, E. de Clercq, A. V. Taichenachev, V. I. Yudin and E. Arimondo, Composite laser-pulses spectroscopy for high-accuracy optical clocks: A review of recent progress and perspectives, Rep. Prog. Phys. **81**, 094401 (2018).

[29] C. Sanner, N. Huntemann, R. Lange, C. Tamm, and E. Peik, Autobalanced Ramsey Spectroscopy, Phys. Rev. Lett. **120**, 053602 (2018).

[30] V. I. Yudin, A. V. Taichenachev, M. Yu. Basalaev, T. Zanon-Willette, J. W. Pollock, M. Shuker, E. A. Donley, and J. Kitching, Generalized Autobalanced Ramsey Spectroscopy of Clock Transitions, Phys. Rev. Appl. **9**, 054034 (2018).

[31] V. I. Yudin, A. V. Taichenachev, M. Yu. Basalaev, T. E. Mehlstäubler, R. Boudot, T. Zanon-Willette, J. W. Pollock, M. Shuker, E. A. Donley, and J. Kitching, Combined error signal in Ramsey spectroscopy of clock transitions, New J. Phys. **20**, 123016 (2018).

[32] M. Abdel Hafiz, G. Coget, M. Petersen, C. Rocher, S. Guérandel, T. Zanon-Willette, E. de Clercq, and R. Boudot, Toward a High-Stability Coherent Population Trapping Cs Vapor-Cell Atomic Clock Using Autobalanced Ramsey Spectroscopy, Phys. Rev. Appl. **9**, 064002 (2018).

[33] M. Abdel Hafiz, G. Coget, M. Petersen, C. E. Calosso, S. Guérandel, E. de Clercq, and R. Boudot, Symmetric autobalanced Ramsey interrogation for high-performance coherentpopulation-trapping vapor-cell atomic clock, Appl. Phys. Lett. **112**, 244102 (2018).

[34] M. Shuker, J. W. Pollock, R. Boudot, V. I. Yudin, A. V. Taichenachev, J. Kitching, and E. A. Donley, Ramsey Spectroscopy with Displaced Frequency Jumps, Phys. Rev. Lett. **122**, 113601 (2019).

[35] M. Shuker, J. W. Pollock, R. Boudot, V. I. Yudin, A. V. Taichenachev, J. Kitching, and E. A. Donley, Reduction of light shifts in Ramsey spectroscopy with a combined error signal, Appl. Phys. Lett. **114**, 141106 (2019).

[36] I. Novikova, Y. Xiao, D. F. Phillips, and R. L. Walsworth, EIT and diffusion of atomic coherence, J. Mod. Opt. **52**, 2381 (2005).

[37] G. A. Pitz, D. E. Wertepny, and G. P. Perram, Pressure broadening and shift of the cesium D_1 transition by the noble gases and N_2, H_2, HD, D_2, CH_4, C_2H_6, CF_4, and ^{3}He, Phys. Rev. A **80**, 062718 (2009).

[38] S. Guérandel, T. Zanon, N. Castagna, F. Dahes, E. de Clercq, N. Dimarcq, and A. Clairon, Raman-Ramsey interaction for coherent population trapping Cs clock, IEEE Trans. Instrum. Meas. **56**, 383 (2007).

[39] P. Yun, Y. Zhang, G. Liu, W. Deng, L. You, and S. Gu, Multipulse Ramsey-CPT interference fringes for the ^{87}Rb clock transition, Europhys. Lett. **97**, 63004 (2012).

[40] Z. Warren, M. S. Shahriar, R. Tripathi, and G. S. Pati, Pulsed coherent population trapping with repeated queries for producing single-peaked high contrast Ramsey interference, J. Appl. Phys. **123**, 053101 (2018).

[41] D. S. Chuchelov, E. A. Tsygankov, S. A. Zibrov, M. I. Vaskovskaya, V. V. Vassiliev, A. S. Zibrov, V. I. Yudin, A. V. Taichenachev, and V. L. Velichansky, Central Ramsey fringe identification by means of an auxiliary optical field, J. Appl. Phys. **126**, 054503 (2019).

[42] T. Zanon-Willette, E. de Clercq, and E. Arimondo, Ultrahigh-resolution spectroscopy with atomic or molecular dark resonances: Exact steady-state line shapes and asymptotic profiles in the adiabatic pulsed regime, Phys. Rev. A **84**, 062502 (2011).